IOP Publishing Journal of Physics: Condensed Matter
J. Phys.: Condens. Matter **27** (2015) 435801 (6pp) doi:10.1088/0953-8984/27/43/435801

Relaxation of electron–hole spins in strained graphene nanoribbons

Sanjay Prabhakar and Roderick Melnik

The MS2Discovery Interdisciplinary Research Institute, M^{2}NeT Laboratory, Wilfrid Laurier University, Waterloo, ON N2L 3C5, Canada

E-mail: sprabhakar@wlu.ca

Received 9 July 2015, revised 3 September 2015
Accepted for publication 17 September 2015
Published 8 October 2015

Abstract

We investigate the influence of magnetic field originating from the electromechanical effect on the spin-flip behaviors caused by electromagnetic field radiation in the strained graphene nanoribbons (GNRs). We show that the spin splitting energy difference (≈10 meV) due to pseudospin is much larger than the spin-orbit coupling effect (Balakrishnan *et al* 2013 *Nat. Phys.* **9** 284) that might provide an evidence of broken symmetry of degeneracy. The induced spin splitting energy due to ripple waves can be further enhanced with increasing values of applied tensile edge stress for potential applications in straintronic devices. In particular, we show that the enhancement in the magnitude of the ripple waves due to externally applied tensile edge stress extends the tuning of spin-flip behaviors to larger widths of GNRs.

Keywords: strained graphene nanoribbon, spin relaxation in graphene nanoribbon, band structure of graphene

(Some figures may appear in colour only in the online journal)

Devices made from graphene are of potential interest for making next generation optoelectronic devices because they possess several noble quantum properties such as the half integer quantum Hall effect and non-zero Berry phase. They can also be useful for the measurement of conductivity of electrons in the electronic devices [1–5]. In addition, the experimentalists observed that this material also carries high mobility charge. Further, one can engineer the straintronic devices by controlling the electromechanical properties via the pseudomorphic gauge fields [6–10]. Photographs taken from high resolution transmission electron microscope or scanning tunneling microscope show that the surface of the graphene sheet is not flat. Its surface varies by several degrees and the out-of-plane deformations reach to the nanometer scale [11–13]. Such out-of-plane deformations or the presence of ripple wave in the surface of graphene can be induced by several different techniques. Most common techniques are either by applying tensile stress or the height fluctuations due to adsorbed hydroxide molecules. Externally applied tensile edge stress might provide the relaxed-shape graphene in the form of torn plastic where a buckling mechanism displaces only the carbon atoms near the edge of the graphene sheet or the height fluctuations throughout the graphene sheet due to adsorbed hydroxide molecules sitting on random sites of hexagon graphene molecules [14, 15]. Such ripples are part of the intrinsic properties of graphene that are expected to strongly affect the band structures due to their coupling through pseudomorphic vector potential [8, 10, 16]. In this paper we present a model that couples the Navier equations, accounting for electromechanical effects, to the electronic properties of GNRs. We show that the ripple waves originating from the electromechanical effects induce large pseudomagnetic fields (for experiments, see [17, 18]) that strongly influence the band structures of GNRs. This response mechanism might be used for tuning the band gaps at the Dirac point in strained GNRs. Numerical estimates of the electromagnetic field mediated spin transition rate in such strained GNRs can be utilized to design the optoelectronic devices for the application in straintronics [19–22].

The total elastic energy density associated with the strain for the two dimensional graphene sheet can be written as [25–27] $2U_s = C_{iklm}\varepsilon_{ik}\varepsilon_{lm}$. Here C_{iklm} is a tensor of rank four (the elastic modulus tensor) and ε_{ik} (or ε_{lm}) is the strain tensor. In the above, we write the strain tensor components for graphene in the 2D displacement vector $\mathbf{u}(x, y) = (u_x, u_y)$ as:

$$\varepsilon_{xx} = \partial_x u_x,\ \varepsilon_{yy} = \partial_y u_y,\ \varepsilon_{xy} = (\partial_y u_x + \partial_x u_y)/2, \qquad (1)$$

where u_x and u_y are the in-plane displacements [14]. The stress tensor components can be easily found from the expression: $\sigma_{ik} = \partial U_s/\partial\varepsilon_{ik}$ and can be written as [28]

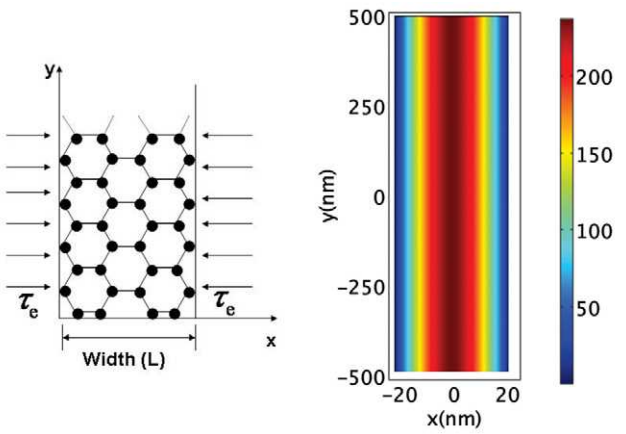

Figure 1. (Left) Schematic diagram of graphene nanoribbon elongated along y-direction and applied tensile edge stress along x-direction. (Right) Spatial dependence of induced magnetic field (strength of the magnetic field expressed in tesla is shown in the color bar) due to variation in strain tensor originating from electromechanical effects in two dimensional GNRs. Here we chose $\tau_e = 45\,\text{eV nm}^{-1}$, $L = 3\sqrt{3}Na$ with $N = 60$ and 1 μm as the length of the ribbon, $c_{11} = 2246.22\,\text{eV nm}^{-2}$ and $\lambda = 2L$. Also see [20, 23].

$$\sigma_{xx} = C_{11}\varepsilon_{xx} + C_{12}\varepsilon_{yy}, \tag{2}$$

$$\sigma_{yy} = C_{12}\varepsilon_{xx} + C_{22}\varepsilon_{yy}, \tag{3}$$

$$\sigma_{xy} = 2C_{66}\varepsilon_{xy}. \tag{4}$$

In the continuum limit, elastic deformations of graphene sheets are described by the Navier equations $\partial_j\sigma_{ik} = 0$. Thus, the two coupled Navier-type equations of electroelasticity in the presence of external forces [25] for two dimensional graphene sheet can be written as:

$$(C_{11}\partial_x^2 + C_{66}\partial_y^2)u_x + (C_{12} + C_{66})\partial_x\partial_y u_y + \frac{F_x}{t} = 0, \tag{5}$$

$$(C_{66}\partial_x^2 + C_{11}\partial_y^2)u_y + (C_{12} + C_{66})\partial_x\partial_y u_x + \frac{F_y}{t} = 0, \tag{6}$$

where t is the thickness of the single layer graphene, $F_x = \partial_x U_x$ and $F_y = \partial_y U_y$ are external forces [25]. Here we assume $U_x = -\tau_e \sin(qx)$ and $U_y = -\tau_e \sin(qy)$ are the externally applied tensile edge energies per unit length. Also $q = 2\pi/\lambda$ with λ being the period length of the in-plane ripple waves. For GNRs elongated along y-direction and applied tensile edge stress only along x-direction i.e. at the zigzag edge along the armchair direction (see figure 1), we only consider ε_{xx} which is a non-vanishing strain tensor component [29][1]. Assuming vanishing displacement vector at $x = \pm L/2$, we write the expression for the displacement vector as:

[1] We may also apply tensile edge stress along the y-direction i.e. at the armchair edge along the zigzag direction (see figure 1) and consider ε_{yy} as non-vanishing strain tensor component. However for this specific case, we find $[H, \varepsilon_{yy}] = 0$. Thus, the y-component of the strain tensor does not induce any quantum confinement effects and may not present much interest from the physics point of view for the design of straintronic devices.

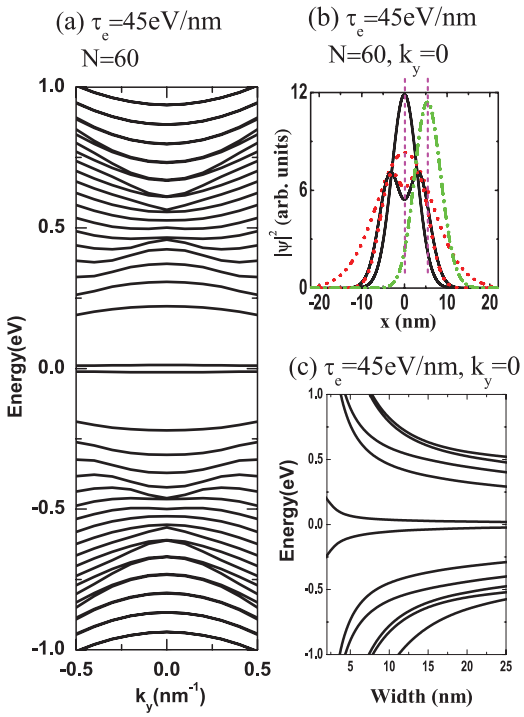

Figure 2. (a,c) Bandstructures of strained GNRs. (b) Dashed-dotted (green) line shows the ground state wave-function for $k_y = -0.3\,\text{nm}^{-1}$ which is shifted from $x = 0$ to $x \approx 5$ nm. The rest of the parameters are chosen the same as in figure 1.

$$u_x = \frac{\tau_e}{qc_{11}t}\left\{\cos\left(\frac{qL}{2}\right) - \cos(qx)\right\}. \tag{7}$$

Now we turn to the influence of strain tensor on the electronic properties of GNRs. In the continuum limit, by expanding the momentum close to the K point in the Brillouin zone, the Hamiltonian for π electrons at the K point reads $H = H_0 + H_z$ as: [2, 30, 31]

$$H = v_F(\sigma_x P_x + \sigma_y P_y) + g_0\mu_B B_s\sigma_z/2, \tag{8}$$

where $P = p - \hbar A$ with $p = -i\hbar\partial_x$ being the canonical momentum operator and $\mathbf{A} = \beta(\varepsilon_{xy}, \varepsilon_{xx} - \varepsilon_{yy}, 0)/a$ being the vector potential induced by pseudomorphic strain tensor [32–35]. The last term is the Zeeman energy, where $B_s = \nabla \times A = B_0 \cos(qx)\hat{z}$ with $B_0 = 2\pi\hbar\beta\tau_e q/ec_{11}ta$ being the effective magnetic field induced by the vector potential. Here a is the lattice constant and $\beta = -\partial \ln t'/\partial \ln a \approx 2$ with t' being the nearest neighbor hoping parameters. Usually the Zeeman energy induced by pseudomagnetic fields is neglected based on the argument that such fields are unable to break the symmetry of degeneracy. However, here we show that the spin splitting energy due to the Zeeman term is much larger than the spin-orbit coupling effect for smaller widths of the GNRs. This might provide an evidence of broken symmetry of degeneracy due to pseudospin originating from ripple waves. By assuming $H\psi = \varepsilon\psi$, where $\psi(r) = \exp(ik_y y)(\phi_A(x)\ \phi_B(x))^T$, [2] we write the two coupled equations as

$$\frac{1}{2}g_0\mu_B B_s\phi_A + \hbar v_F\left(-i\partial_x - ik_y + i\frac{\beta}{a}\varepsilon_{xx}\right)\phi_B = \varepsilon\phi_A, \tag{9}$$

$$\hbar v_{\rm F}\left(-{\rm i}\partial_x+{\rm i}k_y-{\rm i}\frac{\beta}{a}\varepsilon_{xx}\right)\phi_A-\frac{1}{2}g_0\mu_{\rm B}B_s\phi_B=\varepsilon\phi_B. \quad (10)$$

Exact solutions of (9) and (10) are non-trivial. Thus, we seek to apply perturbation theory to get some insight into the behaviors of the band structures of strained GNRs. First, we assume $B_s=B_0\cos(q\hat{x})\approx B_0(1-q^2\hat{x}^2/2!)$ and write the total Hamiltonian $H=\tilde{H}_0+H'_z(\hat{x}^2)$, where

$$\tilde{H}_0=v_{\rm F}(\sigma_x p_x+\sigma_y\hbar k_y-\hbar\sigma_y A_y)+\Delta\sigma_z/2, \quad (11)$$

$$H'_z(\hat{x}^2)=-\Delta q^2\hat{x}^2\sigma_z/4, \quad (12)$$

where $\Delta=g_0\mu_{\rm B}B_0$. Note that the coefficient of σ_z in (11) does not depend on the position operator and it might be impossible to break the symmetry of degeneracy. However, (12) depends on the position operator and below we show that the first order energy correction term of $\tilde{H}_0$ due to H'_z might break the symmetry of degeneracy that can be utilized to induce spin splitting of electron–hole like states for straintronic applications of GNRs. The second order energy correction term of $\tilde{H}_0$ due to H'_z might provide highly asymmetric intra-subband electron–hole spin relaxation in GNRs mediated by electromagnetic field radiation.

We assume $\tilde{H}_0\psi=\tilde{\varepsilon}\psi$ and write two coupled equations associated to (11) as:

$$-{\rm i}\hbar v_{\rm F}(\partial_x+k_y-\beta\varepsilon_{xx}/a)\phi_B=(\tilde{\varepsilon}-\Delta/2)\phi_A, \quad (13)$$

$$-{\rm i}\hbar v_{\rm F}(\partial_x-k_y+\beta\varepsilon_{xx}/a)\phi_A=(\tilde{\varepsilon}+\Delta/2)\phi_B. \quad (14)$$

Now we apply operator $-{\rm i}\hbar v_{\rm F}(\partial_x-k_y+\beta\varepsilon_{xx}/a)$ from left in (13) and write a second order partial differential equation as:

$$(\hbar v_{\rm F})^2\left\{-\partial_x^2+\left(\frac{\beta}{a}\varepsilon_{xx}-k_y\right)^2+\frac{\beta}{a}[\partial_x,\varepsilon_{xx}]\right\}\phi_B=(\tilde{\varepsilon}^2-\Delta^2/4)\phi_B. \quad (15)$$

Evidently from equation (15), the strain tensor provides the parabolic confinement potential whose center shifts from the origin either to the left or to the right by k_y. For example, maxima of the wavefunction shifts to the left for $k_y>0$ and to the right for $k_y<0$ (especially shown in figure 2(b) (dashed-dotted line (green)) for $k_y=-0.3\,{\rm nm}^{-1}$). By utilizing the identity $[x^{\tilde{n}},\partial_x]=-\tilde{n}x^{\tilde{n}-1}$ with $\tilde{n}=1,2,3\cdots$. and considering $\varepsilon_{xx}\approx\tau_e(qx-q^3x^3/3!)/c_{11}t$, we formulate (15) as

$$\left[2m_0v_{\rm F}^2\left(\frac{p_x^2}{2m_0}+\frac{1}{2}m_0\omega_0^2x^2-\tilde{A}\left(x-\frac{q^2x^3}{3!}\right)\right)+A\right]\phi_B=\tilde{\varepsilon}^2\phi_B, \quad (16)$$

where

$$\omega_0=\frac{\hbar}{m_0}\left[\left(\frac{\beta\tau_e q}{c_{11}ta}\right)^2-\frac{\beta\tau_e q^3}{2c_{11}ta}\right]^{1/2}, \quad (17)$$

$$\tilde{A}=\frac{\hbar^2\beta\tau_e qk_y}{m_0c_{11}ta}, A=(\hbar v_{\rm F})^2\left(k_y^2+\frac{\beta\tau_e q}{c_{11}ta}\right)+\frac{\Delta^2}{4}. \quad (18)$$

We treat $-\tilde{A}(x-q^2x^3/3!)$ as a perturbation and write the total energy eigenvalues associated to the Hamiltonian $\tilde{H}_0$ as:

$$\tilde{\varepsilon}_n=\pm\left[2m_0v_{\rm F}^2\left\{\left(n+\frac{1}{2}\right)\hbar\omega_0+\varepsilon_n^{(2)}\right\}+A\right]^{1/2}, \quad (19)$$

where

$$\varepsilon_n^{(2)}=\sum_{m\neq n}\frac{\left|\langle m|-\tilde{A}\hat{x}+\tilde{A}q^2\hat{x}^3/3!|n\rangle\right|^2}{\varepsilon_n^0-\varepsilon_m^0}, \quad (20)$$

$$\langle m|-\tilde{A}\hat{x}+\tilde{A}q^2\hat{x}^3/3!|n\rangle=-\tilde{A}\sqrt{\frac{\hbar}{2m_0\omega_0}}\left(\sqrt{n}\,\delta_{m,n-1}+\sqrt{n+1}\,\delta_{m,n+1}\right)$$
$$+\frac{\tilde{A}q^2}{3!}\left(\frac{\hbar}{2m_0\omega_0}\right)^{3/2}\left(3\sqrt{n^3}\,\delta_{m,n-1}+3\sqrt{(n+1)^3}\,\delta_{m,n+1}+\sqrt{n(n-1)(n-2)}\,\delta_{m,n-3}+\sqrt{(n+1)(n+2)(n+3)}\,\delta_{m,n+3}\right), \quad (21)$$

and $\varepsilon_n^0=(n+1/2)\hbar\omega_0$. Finally by treating H'_z as a perturbation of $\tilde{H}_0$, we write the total energy eigenvalue of H for strained GNRs as:

$$\varepsilon_{n,\sigma_z}=\tilde{\varepsilon}_n+\frac{\Delta q^2\hbar}{8m_0\omega_0}(2n+1)\sigma_z+\left(\frac{\Delta q^2\hbar}{8m_0\omega_0}\right)^2\frac{|\sqrt{(n+1)(n+2)}\,\delta_{m,n+2}+\sqrt{n(n-1)}\,\delta_{m,n-2}+(2n+1)\delta_{m,n}|^2}{\tilde{\varepsilon}_n-\tilde{\varepsilon}_m}. \quad (22)$$

Evidently, the first order energy correction term in (16) gives us the spin splitting of the energy bands of GNRs due to applied tensile edge stress. Assuming the parameters chosen in figure 1 and by utilizing (16), we find the spin splitting energy difference, $\Delta\varepsilon=\varepsilon_{0,+1/2}-\varepsilon_{0,-1/2}=9.1$ meV. Such large spin splitting energy due to ripple waves is much larger

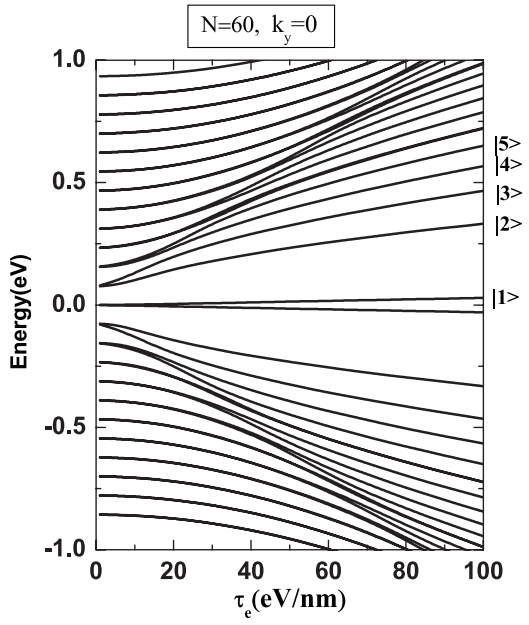

Figure 3. Ripple control of energy eigenvalues of electron–hole like states in a graphene nanoribbon. The parameters are chosen the same as in figure 1.

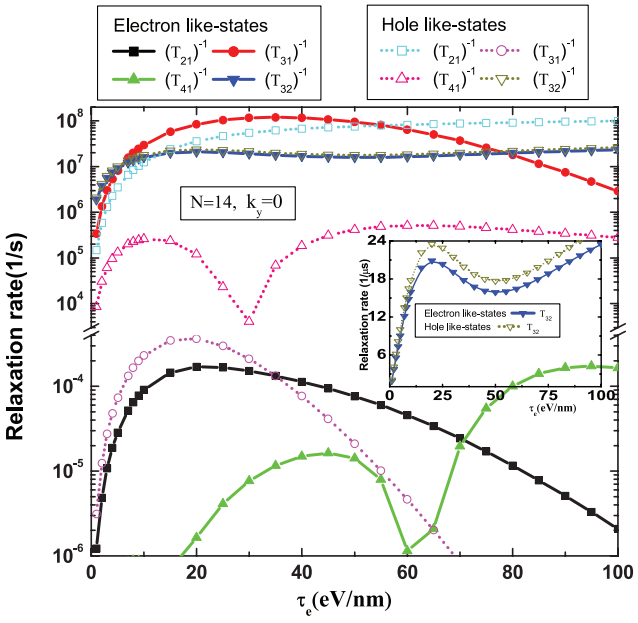

Figure 4. Ripple control of highly asymmetric intra-subband electron–hole relaxation in a relaxed shape graphene nanoribbon. Here T_{21}^{-1} corresponds to the relaxation rate between the states $|2\rangle$ and $|1\rangle$ (also see figure 3 and equation (25)). Similarly, T_{31}^{-1} corresponds to the relaxation rate between the states $|3\rangle$ and $|1\rangle$ and so on. Similar spin relaxation patterns are observed in [24]. The parameters are chosen the same as in figure 1 but $N = 14$.

than the spin-orbit coupling effect (10^{-3} to 2.5 meV) [36] in GNRs. This indicates that the symmetry of degeneracy might be broken due to ripple waves and the Zeeman energy term in the total Hamiltonian of strained GNRs can not be ignored. Accurate solution of the coupled first order differential equations (9) and (10) is done by utilizing the finite element method. We assume that the strain tensor induces parabolic confinement potential in (9) and (10) (also see equation (16)). Thus is also natural to assume vanishing boundary conditions for the wavefunctions at the edges $x = \pm L/2$. For smaller widths of the nanoribbon, the total number of elements in our calculations varies from 157 408 for $L = 3\sqrt{3}aN$ ($N = 2$) to 472 224 for $L = 3\sqrt{3}aN$ ($N = 6$). For larger widths of the ribbon, the total number of elements varies from 19 676 for $L = 3\sqrt{3}aN$ ($N = 8$) to 393 522 for $L = 3\sqrt{3}aN$ ($N = 160$).

In figure 2(a), we plot the dispersion relation $E(k)$ of GNRs. In addition to the band gap of 25 meV at the Dirac point, the localization of the electron–hole wavefunction is shifted from $x = 0$ (solid lines) to $x = 5\,\text{nm}$ for $k_y = -0.3\,\text{nm}^{-1}$ (see dashed-dotted line of figure 2(b)). This is also expected from equation (15) and figure 3 investigates the ripple control of Landau type psedudospin splitting in GNRs. As can be seen, the spin splitting energy is enhanced with applied tensile edge stress along the GNRs due to the enhancement in the induced magnetic fields along z-direction originating from the externally applied tensile edge stress per unit length. Clearly the splitting between the energy states $|1\rangle$ and $|2\rangle$ occurs at low values of the applied tensile edge stress and its value increases linearly for the higher energy states that provide dips in the spin-flip behaviors caused by electromagnetic fields. We address this issues separately in figures 4 and 5 (see below).

We write the total Hamiltonian of graphene under electromagntic field radiation as $\tilde{\tilde{H}} = H + H_{\text{A}}$, where H_{A} is the additional contribution to the Hamiltonian of graphene due to the electromagentic field radiation of photons that can be written as

$$H_{\text{A}} = -ev_{\text{F}}(\sigma_x A_{x,t} + \sigma_y A_{y,t}), \tag{23}$$

where $\mathbf{A}(\mathbf{r}, t)$ is the vector potential of the electromagnetic field radiation of photons that can be written as

$$\mathbf{A}(\mathbf{r}, t) = \sum_{q,\lambda} \sqrt{\frac{\hbar}{2\epsilon_r \omega_{\mathbf{q}} V}}\, \hat{e}_{q\lambda} b_{q,\lambda} \mathrm{e}^{\mathrm{i}(\mathbf{q}\cdot\mathbf{r} - \omega_q t)} + \text{H.c.}, \tag{24}$$

where $\omega_q = c|\mathbf{q}|$, $b_{q,\lambda}$ annihilate photons with wave vector $\mathbf{q}$, c is the velocity of light, V is the volume and ϵ_r is the dielectric constant of the graphene nanoribbon. The polarization directions $\hat{e}_{\mathbf{q}\lambda}$ with $\lambda = 1, 2$ are chosen as two perpendicular induced photon modes in the graphene nanoribbon. The polarization directions of the induced photon are $\hat{e}_{q1} = (\sin\phi, -\cos\phi, 0)$ and $\hat{e}_{q2} = (\cos\theta\cos\phi, \cos\theta\sin\phi, -\sin\theta)$ because we express $\mathbf{q} = q(\sin\theta\cos\phi, \sin\theta\sin\phi, \cos\theta)$. The above polarization vectors satisfy the relations $\hat{e}_{q1} = \hat{e}_{q2} \times \hat{\mathbf{q}}$, $\hat{e}_{q2} = \hat{\mathbf{q}} \times \hat{e}_{q1}$ and $\hat{\mathbf{q}} = \hat{\mathbf{e}}_{\mathbf{q}1} \times \hat{\mathbf{e}}_{\mathbf{q}2}$. Based on the Fermi Golden Rule, the electromagnetic field mediated transition rate (i.e. the transition probability per unit time) in the graphene nanoribbon is given by [37]

$$\frac{1}{T_{fi}} = \frac{V}{(2\pi)^2\hbar} \int d^3\mathbf{q} \sum_{\lambda=1,2} |M_{q,\lambda}|^2 \delta(\hbar\omega_{\mathbf{q}} - \varepsilon_f + \varepsilon_i), \tag{25}$$

where $M_{q,\lambda} = \langle\psi_i|H_{\text{A}}|\psi_f\rangle$. Here $|\psi_i\rangle$ and $|\psi_f\rangle$ are the initial and final states wavefunctions. By adopting the dipole approximation, i.e. by assuming that the transition is caused only by leading terms from $A(\mathbf{r}t)$, we plotted the electromagnetic field

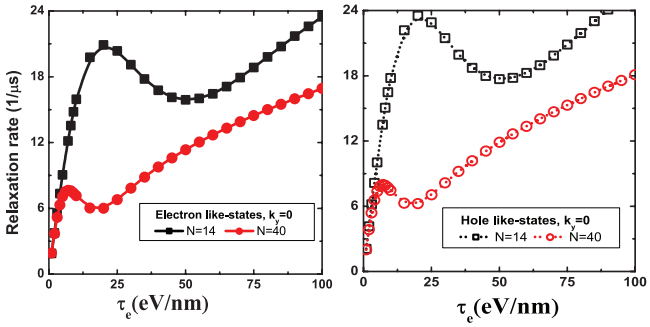

Figure 5. Ripple control of highly asymmetric intra-subband electron–hole relaxation ($|3\rangle \rightarrow |2\rangle$) in a relaxed shape graphene nanoribbon. Here we chose $L = 3\sqrt{3}\,aN$, $c_{11} = 2246.22\,\text{eV nm}^{-2}$ and $\lambda = 2L$.

mediated spin relaxation rate versus externally applied tensile edge stress per unit length in figures 4 and 5.

In figure 4, we plot ripple control of highly asymmetric electron–hole spin relaxation in strained GNRs. The numerical estimate of spin relaxation rate is in agreement to the experimentally reported results in [38]. The highly asymmetric electron–hole relaxation can be observed due to the presence of higher order terms that depend on the position operators in the Zeeman term of (8). For quantum information processing, we need larger transition times for gate operation. Thus the transition rates ($10^{-8}\,\text{s}^{-1}$ to $10^{-3}\,\text{s}^{-1}$) (for experiment, also see [38]) shown in the lower panel of figure 4 might provide ideal states in GNRs for gate operation before reaching decoherence for quantum information and quantum computing (also see [24]). In figure 5, we plot electron–hole relaxation rate versus the applied tensile edge stress per unit length for GNRs of widths $L = 10.3\,\text{nm}$ (squares) and $L = 29.5\,\text{nm}$ (circles). By precisely examining the numerical estimate, we again see the highly asymmetric electron–hole relaxation due to the presence of higher order terms depending on the position operator in the Zeeman energy term. In both highly asymmetric electron–hole transition rates, we clearly see that the tuning point (i.e. dips in the transition rate) extends to smaller widths of the GNRs. The tuning point (dip) in the transition rate can be seen due to the crossing of the energy bands associated to the states $|2\uparrow\rangle$ and $|3\downarrow\rangle$. In other words, we expect the level crossing point in a location where $\varepsilon_{2\uparrow} = \varepsilon_{3\downarrow}$. Assuming that the last term in (22) is much smaller than $\tilde{\varepsilon}_n$, we write the condition for the tuning point as:

$$\sqrt{\frac{8\beta\tau_e q}{c_{11}ta}}\left[1+\frac{1}{32}\left(\frac{2\pi g_0\mu_B}{ev_F}\right)^2\left(\frac{\beta\tau_e q}{c_{11}ta}\right)\right]^{1/2} - \sqrt{\frac{6\beta\tau_e q}{c_{11}ta}}\left[1+\frac{1}{24}\left(\frac{2\pi g_0\mu_B}{ev_F}\right)^2\left(\frac{\beta\tau_e q}{c_{11}ta}\right)\right]^{1/2} = \frac{3\pi}{ev_F}g_0\mu_B q^2. \tag{26}$$

For simplicity in equation (26), we consider $\omega_0 = \hbar\beta\tau_e q/m_0 c_{11}ta$ because we assume $\pi^2/2L^2 \ll 1$ in equation (17) for $N = 14$ and $N = 40$ which is the choice of the ribbon width in figure 5. Finally, the second term in the square bracket of equation (26) is also much smaller than unity. By considering $q = 2\pi/\lambda$ with $\lambda = 2L$, we write the expression for τ_e at the tuning point (dip) in terms of graphene nanoribbon width as:

$$\tau_e = \frac{\pi^3 C}{L^3}, \tag{27}$$

where the constant

$$C = \left(\frac{2\pi g_0\mu_B}{ev_F}\right)^2 \frac{c_{11}ta}{\beta\left(14-8\sqrt{3}\right)}. \tag{28}$$

Hence in equation (27), we see that the applied tensile edge stress is inversely proportional to the width of the GNRs at the tuning point (dip) that is reflected in figure 5.

To conclude, we have provided an idea of inducing large anisotropic Zeeman energies in strained GNRs (see figure 1). Based on the exact diagonalization and second order perturbation theory, we have shown that it is possible to find the large pseudospin splitting energy difference due to ripple waves. Such spin splitting energy is much larger than the spin-orbit coupling effect that might provide an evidence of broken symmetry of degeneracy. Finally, in figures 4 and 5, our numerical estimates of relaxation times among several energy states might be further considered to assist in manipulating spin for making next generation straintronic devices for quantum information processing and quantum computing.

Acknowledgments

We acknowledge NSERC and CRC programs (Canada) for their financial support.

References

[1] Das Sarma S, Adam S, Hwang E H and Rossi E 2011 *Rev. Mod. Phys.* **83** 407
[2] Castro Neto A H, Guinea F, Peres N M R, Novoselov K S and Geim A K 2009 *Rev. Mod. Phys.* **81** 109
[3] Novoselov K S, Geim A K, Morozov S V, Jiang D, Katsnelson M I, Grigorieva I V, Dubonos S V and Firsov A A 2005 *Nature* **438** 197
[4] Novoselov K S, Jiang D, Schedin F, Booth T J, Khotkevich V V, Morozov S V and Geim A K 2005 *Proc. Natl Acad. Sci.* **102** 10451
[5] Novoselov K S, Geim A K, Morozov S V, Jiang D, Zhang Y, Dubonos S V, Grigorieva I V and Firsov A A 2004 *Science* **306** 666
[6] Shenoy V B, Reddy C D, Ramasubramaniam A and Zhang Y W 2008 *Phys. Rev. Lett.* **101** 245501
[7] Choi S-M, Jhi S-H and Son Y-W 2010 *Phys. Rev.* B **81** 081407
[8] Bao W, Myhro K, Zhao Z, Chen Z, Jang W, Jing L, Miao F, Zhang H, Dames C and Lau C N 2012 *Nano Lett.* **12** 5470
[9] Cadelano E, Palla P L, Giordano S and Colombo L 2009 *Phys. Rev. Lett.* **102** 235502
[10] Bao W, Miao F, Chen Z, Zhang H, Jang W, Dames C and Lau C N 2009 *Nat. Nano* **4** 562
[11] Meyer J C, Geim A K, Katsnelson M I, Novoselov K S, Booth T J and Roth S 2007 *Nature* **446** 60
[12] Bonilla L L and Carpio A 2012 *Phys. Rev.* B **86** 195402
[13] Guinea F, Katsnelson M I and Geim A K 2010 *Nat. Phys.* **6** 30

[14] Prabhakar S, Melnik R, Bonilla L L and Badu S 2014 *Phys. Rev.* B **90** 205418
[15] Fasolino A, Los J H and Katsnelson M I 2007 *Nat. Mater.* **6** 858
[16] Cerda E and Mahadevan L 2003 *Phys. Rev. Lett.* **90** 074302
[17] Klimov N N, Jung S, Zhu S, Li T, Wright C A, Solares S D, Newell D B, Zhitenev N B and Stroscio J A 2012 *Science* **336** 1557
[18] Zhu S, Huang Y, Klimov N N, Newell D B, Zhitenev N B, Stroscio J A, Solares S D and Li T 2014 *Phys. Rev.* B **90** 075426
[19] Levy N, Burke S A, Meaker K L, Panlasigui M, Zettl A, Guinea F, Neto A H C and Crommie M F 2010 *Science* **329** 544
[20] Moldovan D, Ramezani Masir M and Peeters F M 2013 *Phys. Rev.* B **88** 035446
[21] He W-Y, Su Y, Yang M and He L 2014 *Phys. Rev.* B **89** 125418
[22] San-Jose P, Prada E, McCann E and Schomerus H 2009 *Phys. Rev. Lett.* **102** 247204
[23] Neek-Amal M and Peeters F M 2010 *Phys. Rev.* B **82** 085432
[24] Droth M and Burkard G 2013 *Phys. Rev.* B **87** 205432
[25] Landau L D and Lifshitz E M 1970 *Theory of Elasticity* (Oxford: Pergamon)
[26] Carpio A and Bonilla L L 2008 *Phys. Rev.* B **78** 085406
[27] Cadelano E and Colombo L 2012 *Phys. Rev.* B **85** 245434
[28] Zhou J and Huang R 2008 *J. Mech. Phys. Solids* **56** 1609
[29] Meng L *et al* 2013 *Phys. Rev.* B **87** 205405
[30] Maksym P A and Aoki H 2013 *Phys. Rev.* B **88** 081406
[31] Krueckl V and Richter K 2012 *Phys. Rev.* B **85** 115433
[32] Kitt A L, Pereira V M, Swan A K and Goldberg B B 2012 *Phys. Rev.* B **85** 115432
[33] Guinea F, Katsnelson M I and Vozmediano M A H 2008 *Phys. Rev.* B **77** 075422
[34] Guinea F, Horovitz B and Le Doussal P 2008 *Phys. Rev.* B **77** 205421
[35] de Juan F, Mañes J L and Vozmediano M A H 2013 *Phys. Rev.* B **87** 165131
[36] Balakrishnan J, Kok Wai Koon G, Jaiswal M, Castro Neto A H and Ozyilmaz B 2013 *Nat. Phys.* **9** 284
[37] Merzbacher E 2004 *Quantum Mechanics* (New York: Wiley)
[38] Guimarães M H D, Zomer P J, Ingla-Aynés J, Brant J C, Tombros N and van Wees B J 2014 *Phys. Rev. Lett.* **113** 086602